

# Search for ${}^6_{\Lambda}\text{H}$ hypernucleus by the ${}^6\text{Li}(\pi^-, K^+)$ reaction at $p_{\pi^-} = 1.2 \text{ GeV}/c$

H. Sugimura<sup>a,b,\*</sup>, M. Agnello<sup>c,d</sup>, J.K. Ahn<sup>e</sup>, S. Ajimura<sup>f</sup>, Y. Akazawa<sup>g</sup>, N. Amano<sup>a</sup>, K. Aoki<sup>h</sup>, H.C. Bhang<sup>i</sup>, N. Chiga<sup>g</sup>, M. Endo<sup>j</sup>, P. Evtoukhovitch<sup>k</sup>, A. Feliciello<sup>d</sup>, H. Fujioka<sup>a</sup>, T. Fukuda<sup>l</sup>, S. Hasegawa<sup>b</sup>, S. Hayakawa<sup>j</sup>, R. Honda<sup>g</sup>, K. Hosomi<sup>g</sup>, S.H. Hwang<sup>b</sup>, Y. Ichikawa<sup>a,b</sup>, Y. Igarashi<sup>h</sup>, K. Imai<sup>b</sup>, N. Ishibashi<sup>j</sup>, R. Iwasaki<sup>h</sup>, C.W. Joo<sup>i</sup>, R. Kiuchi<sup>i,b</sup>, J.K. Lee<sup>e</sup>, J.Y. Lee<sup>i</sup>, K. Matsuda<sup>j</sup>, Y. Matsumoto<sup>g</sup>, K. Matsuoka<sup>j</sup>, K. Miwa<sup>g</sup>, Y. Mizoi<sup>l</sup>, M. Moritsu<sup>f</sup>, T. Nagae<sup>a</sup>, S. Nagamiya<sup>b</sup>, M. Nakagawa<sup>j</sup>, M. Naruki<sup>a</sup>, H. Noumi<sup>f</sup>, R. Ota<sup>j</sup>, B.J. Roy<sup>m</sup>, P.K. Saha<sup>b</sup>, A. Sakaguchi<sup>j</sup>, H. Sako<sup>b</sup>, C. Samanta<sup>n</sup>, V. Samoilov<sup>k</sup>, Y. Sasaki<sup>g</sup>, S. Sato<sup>b</sup>, M. Sekimoto<sup>h</sup>, Y. Shimizu<sup>l</sup>, T. Shiozaki<sup>g</sup>, K. Shirotori<sup>f</sup>, T. Soyama<sup>j</sup>, T. Takahashi<sup>h</sup>, T.N. Takahashi<sup>o</sup>, H. Tamura<sup>g</sup>, K. Tanabe<sup>g</sup>, T. Tanaka<sup>j</sup>, K. Tanida<sup>i</sup>, A.O. Tokiyasu<sup>f</sup>, Z. Tsamalaidze<sup>k</sup>, M. Ukai<sup>g</sup>, T.O. Yamamoto<sup>g</sup>, Y. Yamamoto<sup>g</sup>, S.B. Yang<sup>i</sup>, K. Yoshida<sup>j</sup>,  
(J-PARC E10 Collaboration)

<sup>a</sup>Department of Physics, Kyoto University, Kyoto 606-8502, Japan

<sup>b</sup>Japan Atomic Energy Agency(JAEA), Tokai, Ibaraki 319-1195, Japan

<sup>c</sup>Dipartimento di Scienza Applicata e Tecnologia, Politecnico di Torino, I-10129, Torino, Italy

<sup>d</sup>INFN, Istituto Nazionale di Fisica Nucleare, Sez. di Torino I-10125, Torino, Italy

<sup>e</sup>Department of Physics, Pusan National University, Busan 609-735, Republic of Korea

<sup>f</sup>Research Center for Nuclear Physics (RCNP), 10-1 Mihogaoka, Ibaraki, Osaka 567-0047, Japan

<sup>g</sup>Department of Physics, Tohoku University, Sendai 980-8578, Japan

<sup>h</sup>High Energy Accelerator Research Organization (KEK), Tsukuba 305-0801, Japan

<sup>i</sup>Department of Physics and Astronomy, Seoul National University, Seoul 151-747, Republic of Korea

<sup>j</sup>Department of Physics, Osaka University, Toyonaka, Osaka 560-0043, Japan

<sup>k</sup>Joint Institute for Nuclear Research, Dubna, Moscow Region 141980, Russia

<sup>l</sup>Department of Engineering Science, Osaka Electro-Communication University, Neyagawa, Osaka 572-8530, Japan

<sup>m</sup>Nuclear Physics Division, Bhabha Atomic Research Center (BARC), Trombay, Mumbai 400 085, India

<sup>n</sup>Department of Physics and Astronomy, Virginia Military Institute, Lexington, VA 24450, USA

<sup>o</sup>RIKEN, 2-1 Hirosawa, Wako, Saitama 351-0198, Japan

arXiv:1310.6104v2 [nucl-ex] 6 Feb 2014

## Abstract

We have carried out an experiment to search for a neutron-rich hypernucleus,  ${}^6_{\Lambda}\text{H}$ , by the  ${}^6\text{Li}(\pi^-, K^+)$  reaction at  $p_{\pi^-} = 1.2 \text{ GeV}/c$ . The obtained missing-mass spectrum with an estimated energy resolution of 3.2 MeV (FWHM) showed no peak structure corresponding to the  ${}^6_{\Lambda}\text{H}$  hypernucleus neither below nor above the  ${}^4_{\Lambda}\text{H}+2n$  particle decay threshold. An upper limit of the production cross section for the bound  ${}^6_{\Lambda}\text{H}$  hypernucleus was estimated to be 1.2 nb/sr at 90% confidence level.

**Keywords:** Neutron-rich  $\Lambda$ -hypernuclei, Missing-mass spectroscopy

## 1. Introduction

Since the first discovery of a cosmic-ray induced hyperfragment formation event in emulsion [1], various  $\Lambda$ -hypernuclei have been observed. Especially, extensive studies have been made by missing-mass spectroscopy with magnetic spectrometers by using the  $(K^-, \pi^-)$  and  $(\pi^+, K^+)$  reactions [2, 3, 4, 5], and the properties of the  $\Lambda N$  interaction have been extracted from the level structures of the  $\Lambda$ -hypernuclei. Furthermore, details of the spin-dependent interactions have been studied by  $\gamma$ -ray spectroscopy with germanium and NaI detectors [6, 7, 8].

When we embed a  $\Lambda$  hyperon in a nucleus, there are several interesting features theoretically expected for some specific hypernuclei. One example is the glue-like role of a  $\Lambda$  hyperon in the hypernuclei. Unstable nuclei such as  ${}^8\text{Be}$  become stable against the particle decays by adding a  $\Lambda$  hyperon. The

glue-like role gives a critical contribution to the binding especially around the proton- and neutron-drip lines, and may extend the boundary of stability of nuclei. Another example is a large effect of the  $\Lambda N$ - $\Sigma N$  mixing which was first discussed by Gibson et al. for  $s$ -shell  $\Lambda$ -hypernuclei [9]. The idea has been extended to the coherent  $\Lambda N$ - $\Sigma N$  mixing by Akaishi et al. to understand the binding energies of  $s$ -shell  $\Lambda$ -hypernuclei systematically [10]. A non-zero isospin of the core nucleus is essential for the large mixing because the core nucleus is a buffer of the isospin to compensate the isospin difference between  $\Lambda$  and  $\Sigma$ . The studies on the neutron-rich  $\Lambda$ -hypernuclei with a large isospin are important to understand the properties of the  $\Lambda N$ - $\Sigma N$  mixing effect.

The highly neutron-rich  $\Lambda$ -hypernucleus  ${}^6_{\Lambda}\text{H}$  was first discussed by Dalitz and Levi-Setti [11]. They predicted the  $\Lambda$ -binding energy of the ground state to be 4.2 MeV based on the knowledge of the core nucleus  ${}^5\text{H}$  at that time. Later on, Korshennikov et al. reported an observation of the  ${}^5\text{H}$  ground state as a resonant state unbound by 1.7 MeV with respect to

\*Corresponding author. Tel:+81 29 2825457

Email address: sugimura@sphys.kyoto-u.ac.jp (H. Sugimura)

the  $t + 2n$  threshold [12]. Including the new experimental information, there were extensive theoretical discussions on the structure of  ${}^6_{\Lambda}\text{H}$ . Akaishi et al. suggested a considerably large binding energy of 5.8 MeV for the  $0^+$  ground state due to rather large contribution of 1.4 MeV from the coherent  $\Lambda\text{N}$ - $\Sigma\text{N}$  mixing [13]. Gal and Millener predicted a binding energy of  $(3.83 \pm 0.08 \pm 0.22)$  MeV by a shell-model calculation [14]. Hiyama et al. performed  $t + n + n + \Lambda$  four-body cluster-model calculation, which reproduced the properties of  ${}^5\text{H}$  as well, and obtained a binding energy of 2.47 MeV [15]. These theoretically estimated binding energies were distributed from bound to unbound regions with respect to the  ${}^4\text{H} + 2n$  particle decay threshold, which corresponded to a  $\Lambda$ -binding energy of 3.74 MeV, and were quite sensitive to the  $\Lambda\text{N}$  interaction and the properties of the core nucleus  ${}^5\text{H}$ .

The double charge-exchange (DCX) reactions, such as the  $(K^-, \pi^+)$  and the  $(\pi^-, K^+)$  reactions, are promising spectroscopic tools to access the  $\Lambda$ -hypernuclei close to the neutron drip-line [16]. The first study of the neutron-rich  $\Lambda$ -hypernuclei with the DCX reaction was performed at the KEK proton synchrotron facility by using the  $(K^-_{\text{stopped}}, \pi^+)$  reaction, and upper limits of the production cross sections for several neutron-rich  $\Lambda$ -hypernuclei were provided [17]. Another DCX reaction, the  ${}^{10}\text{B}(\pi^-, K^+)$  reaction at 1.2 GeV/c, was measured in the KEK-E521 experiment [18]. Since there was no physical background in the  $(\pi^-, K^+)$  reaction, the  ${}^{10}_{\Lambda}\text{Li}$  production events were clearly observed in the  $\Lambda$  bound region. The production cross section was reported  $(11.3 \pm 1.9)$  nb/sr which was roughly  $10^{-3}$  of that of the non charge-exchange  $(\pi^+, K^+)$  reaction. Possible reaction mechanisms of the  $(\pi^-, K^+)$  reaction were discussed by Harada et al. from a theoretical point of view [19]. The FINUDA collaboration also measured the  $(K^-_{\text{stopped}}, \pi^+)$  reaction [20] and recently reported three candidate events of  ${}^6_{\Lambda}\text{H}$  by the simultaneous measurement of both the production and the mesonic weak decay processes of  ${}^6_{\Lambda}\text{H}$  [21]. The FINUDA collaboration reported a binding energy for  ${}^6_{\Lambda}\text{H}$  close to the Dalitz and Levi-Setti calculation. However, because of the small number of the candidate events, the FINUDA observation should be confirmed with higher statistics.

## 2. J-PARC E10 experiment

The J-PARC E10 experiment was proposed to produce the neutron-rich  $\Lambda$ -hypernucleus  ${}^6_{\Lambda}\text{H}$  by using the  ${}^6\text{Li}(\pi^-, K^+)$  reaction at 1.2 GeV/c and to study its structure. The experiment is performed at the K1.8 beam line of J-PARC Hadron Experimental Facility. The K1.8 beam line spectrometer [22] and the Superconducting Kaon Spectrometer (SKS) [22, 23] are used after modifications to cope with the high beam intensity, more than  $10^7$  pions per spill (2s duration) occurring every 6s, which is necessary to override the tiny production cross section. Figure 1 shows the K1.8 beam line and the SKS spectrometers.

The K1.8 beam line spectrometer consists of a gas Čerenkov counter (GC), a scintillating fiber tracker (BFT), QQDQQ magnets, two drift chambers (BC3 and BC4) and a timing plastic scintillation hodoscope (BH2). BFT is a scintillating fiber

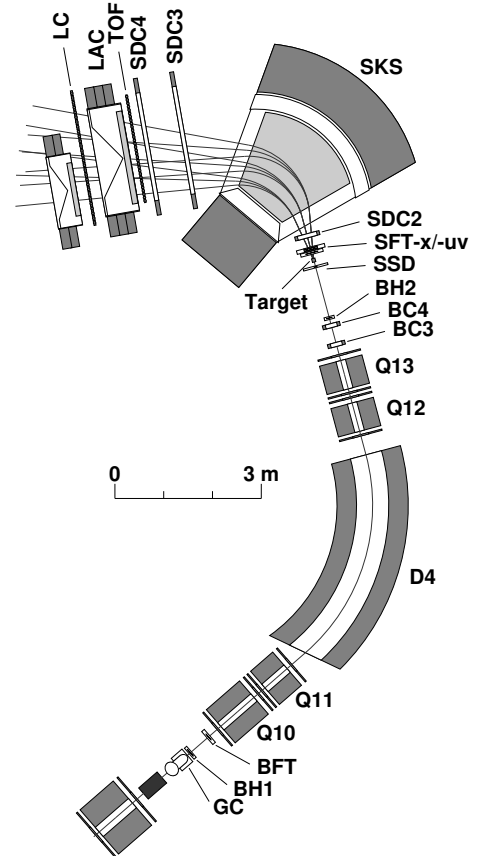


Figure 1: Schematic view of the K1.8 beam line spectrometer (from GC to BH2), the target area (SSD and Target) and the SKS spectrometer (from SFT to LC). See the text for more details.

tracker with a  $xx'$  structure and is made of scintillating fibers with 1 mm diameter. The light signals from the scintillating fibers are read out by MPPCs (Multi Pixel Photon Counters) and the EASIROC system [24]. The time resolution is 0.86 ns (rms) which is good enough to reduce accidental hits due to the high rate beams. BC3 and BC4 are 3 mm wire pitch drift chambers. BH2 is a timing plastic scintillator placed at the exit of the K1.8 beam line spectrometer. BH2 defines the start timing of the readout and the DAQ systems and counts the number of incoming pions. The time resolution of BH2 is 90 ps (rms). The pion beam momentum is reconstructed to an accuracy of  $3.3 \times 10^{-4}$  (FWHM) by using a 3rd-order transfer matrix and the hit position information from BFT, BC3, and BC4.

An enriched  ${}^6\text{Li}$  target (95.54%) of  $3.5 \text{ g/cm}^2$  in thickness, 70 mm in width and 40 mm in height is used. The typical beam profile, 56 mm in horizontal and 28 mm in vertical (FWTM), is fully covered with the target. To reconstruct the reaction vertex point precisely and to find the right combination of upstream and downstream tracks for multi-track events, silicon strip detectors (SSD), with a  $80 \mu\text{m}$  strip pitch, are installed just upstream the target.

The SKS spectrometer consists of a scintillating fiber tracker (SFT), three drift chambers (SDC2, SDC3 and SDC4), a superconducting magnet, a timing plastic scintillation hodoscope (TOF) and two threshold-type Čerenkov counters (LAC and

LC). The SKS magnetic field is 2.16 T and the momentum acceptance of the SKS spectrometer ranges from 0.7 to 1.4 GeV/c. The kaon momentum from the  ${}^6\text{Li}(\pi^-, K^+){}^6_\Lambda\text{H}$  reaction is around 0.9 GeV/c, while the angular acceptance of the SKS spectrometer is roughly 100 msr at that momentum. SFT is a scintillating fiber tracker with a  $xx'vu$  structure. The  $x$  and  $x'$  planes have a similar structure of BFT. The  $v$  and  $u$  planes tilted by 45 degrees are made of scintillating fibers with 0.5 mm diameter. The time resolutions are 0.87 ns and 1.17 ns (rms) for the  $xx'$  and  $uv$  planes, respectively. SDC2 is a 5 mm wire pitch drift chamber. SFT and SDC2 are placed at the entrance of the SKS magnet. SDC3 and SDC4 are 20 mm wire pitch drift chambers placed at the exit of the SKS magnet. TOF is a timing plastic scintillator and the timing resolution is 85 ps (rms). LAC and LC are threshold-type Čerenkov counters with a  $n=1.05$  silica aerogel and a  $n=1.49$  acrylic radiators, respectively. Kaons do not exceed the Čerenkov threshold of LAC and exceed the threshold of LC for the momentum range covered by SKS. The scattered particle momentum is reconstructed to an accuracy of 0.1% (FWHM) by using Runge-Kutta integration method with the hit position information of SFT, SDC2, SDC3 and SDC4.

The on-line trigger for the measurements of the  $(\pi^\pm, K^+)$  reactions consists of the 1st level trigger defined as  $\text{BH2} \times \text{TOF} \times \overline{\text{LAC}} \times \text{LC}$  and the 2nd level trigger to reduce proton backgrounds by using the  $\text{BH2-TOF}$  time-of-flight information. The data are taken by a network based DAQ system, HDDAQ [25], which integrates several kinds of conventional DAQ subsystems.

### 3. Results

Table 1 shows a summary of runs of the J-PARC E10 experiment. Before the measurement of the DCX reaction on the  ${}^6\text{Li}$  target, we measured the  ${}^{12}\text{C}(\pi^+, K^+){}^{12}_\Lambda\text{C}$  reaction at the beam momentum of 1.2 GeV/c to evaluate the missing-mass resolution in a kinematical condition close to that of the  ${}^6\text{Li}(\pi^-, K^+){}^6_\Lambda\text{H}$  reaction. A graphite target of 3.6 g/cm<sup>2</sup> in thickness was used, and the beam intensity was  $4.1 \times 10^6$  pion/spill. Figure 2 shows the excitation energy spectrum of the  ${}^{12}_\Lambda\text{C}$  hypernucleus obtained from the measurement. The ground ( $s_\Lambda$ ) and excited ( $p_\Lambda$ ) states of the  ${}^{12}_\Lambda\text{C}$  hypernucleus are clearly observed. The ground state region is fitted with three Gaussian functions corresponding to the ground and to known excited states at 2.833 and 6.050 MeV [26, 27]. A same width of the Gaussian function is used for the three states. The missing-mass resolution is estimated to be 3.2 MeV (FWHM).

We performed the pion beam-through runs at four momentum settings, 0.8, 0.9, 1.0 and 1.2 GeV/c, without the target to evaluate the momentum difference between the K1.8 beam line and the SKS spectrometers. We also measured the  $p(\pi^-, K^+)\Sigma^-$  and the  $p(\pi^+, K^+)\Sigma^+$  reactions at 1.377 GeV/c to calibrate the beam momentum with a  $(\text{CH}_2)_n$  target of 3.4 g/cm<sup>2</sup> in thickness. The pion beam momentum 1.377 GeV/c was selected so that the produced  $K^+$  momentum in the  $p(\pi^\pm, K^+)\Sigma^\pm$  reaction coincides with that in the  ${}^6\text{Li}(\pi^-, K^+){}^6_\Lambda\text{H}$  reaction at 1.2 GeV/c. The beam intensities in the  $\Sigma^-$  and  $\Sigma^+$  production runs were  $1.3 \times 10^7$  and  $3.5 \times 10^6$  pion/spill, respectively. The momenta

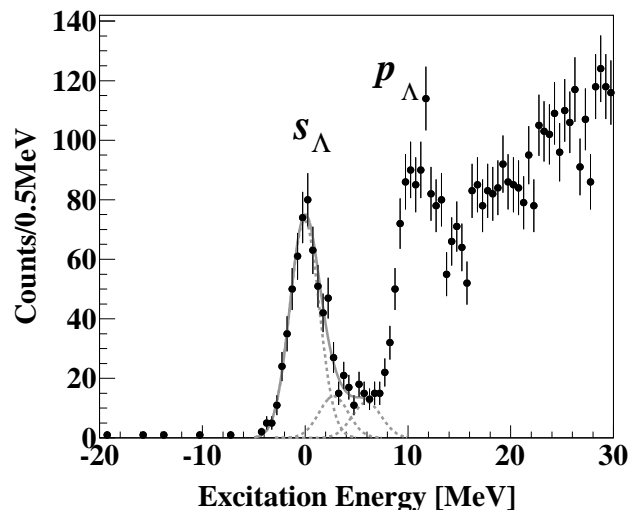


Figure 2: Excitation energy spectrum of the  ${}^{12}\text{C}(\pi^+, K^+){}^{12}_\Lambda\text{C}$  reaction at the beam momentum of 1.2 GeV/c. The ground ( $s_\Lambda$ ) and excited ( $p_\Lambda$ ) states are clearly observed. The missing-mass resolution is estimated by fitting the ground and known excited states. The dashed curves show the best fit Gaussian functions for these states and the solid curve is the sum.

of particles measured by the K1.8 beam line spectrometer are corrected with a 1st-order polynomial function by considering the results of the beam-through run at 0.9 GeV/c and the  $\Sigma^+$  production reaction. Furthermore, the effect of the beam polarity change from  $\pi^+$  to  $\pi^-$  to the missing-mass is evaluated by the  $\Sigma^-$  production reaction. The momenta of scattered particles measured by the SKS spectrometer are not corrected because the SKS magnetic field is fixed in all runs. In the case of the 1.2 GeV/c beam momentum used in the  ${}^6\text{Li}(\pi^-, K^+)$  reaction measurement, the amount of the momentum correction is  $-1.2$  MeV/c. The systematic uncertainty of the beam momentum is estimated from the beam-through runs at 0.8, 1.0 and 1.2 GeV/c after the momentum correction. The momentum differences after the correction are  $-1.46$ ,  $+1.62$ , and  $-0.79$  MeV/c at 0.8, 1.0, and 1.2 GeV/c, respectively. From these values, the systematic uncertainty is estimated to be  $\pm 1.34$  MeV/c.

We performed the measurement of the  ${}^6\text{Li}(\pi^-, K^+)$  reaction at the beam momentum of 1.2 GeV/c. We used high intensity beams of  $1.2\text{--}1.4 \times 10^7$  pion/spill and the effective total number of beam pions on the target was  $1.4 \times 10^{12}$  taking into account the DAQ efficiency. Since the  $(\pi^-, K^+)$  reaction has no physical background and the cross section of the reaction is very small, contaminations from the miss-identification of  $\pi^+$  and proton are the source of the backgrounds. Figure 3 shows the mass squared vs momentum plot of the particles measured by the SKS spectrometer. We selected kaons by a momentum dependent cut at  $\pm 2\sigma$  of the mass squared resolution as indicated with curves in the figure. The contamination of protons in the  $K^+$  cut region is at 1% level in the momentum range of 0.68–1.2 GeV/c, and the contamination of  $\pi^+$  is negligibly small.

For quantitative discussions of the  ${}^6\text{Li}(\pi^-, K^+)$  reaction, the double differential cross section is derived from the following

Table 1: Summary of runs. Target material and thickness, and beam momentum and intensity are listed.

run	target		beam	
	material	thickness (g/cm <sup>2</sup> )	momentum (GeV/c)	intensity (pion/spill)
<sup>6</sup> Li( $\pi^-$ , $K^+$ )	<sup>6</sup> Li (95.54% enriched)	3.5	1.2	$1.2-1.4 \times 10^7$
<sup>12</sup> C( $\pi^+$ , $K^+$ )	graphite	3.6	1.2	$4.1 \times 10^6$
$p(\pi^-, K^+)\Sigma^-$	(CH <sub>2</sub> ) <sub>n</sub>	3.4	1.377	$1.3 \times 10^7$
$p(\pi^+, K^+)\Sigma^+$	(CH <sub>2</sub> ) <sub>n</sub>	3.4	1.377	$3.5 \times 10^6$
beam-through	none		0.8, 0.9, 1.0, 1.2	$\sim 10^4$

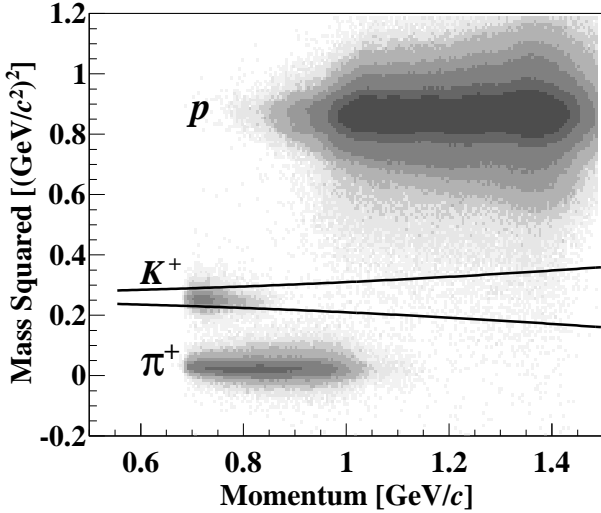


Figure 3: Mass squared vs. momentum plot of the scattered particles measured by the SKS spectrometer in the <sup>6</sup>Li( $\pi^-$ ,  $K^+$ ) reaction. Two curves in the figure show the momentum dependent  $2\sigma$  cut for the kaon selection.

equation,

$$\frac{d^2\sigma}{d\Omega dM} = \frac{A}{N_A \rho x} \frac{n_K}{N_{\text{beam}} \Delta\Omega \Delta M \epsilon}, \quad (1)$$

where  $n_K$  is the number of detected kaons in the missing-mass interval  $\Delta M$ .  $N_A$  is the Avogadro number, and  $A$  and  $\rho x$  are the atomic mass and the thickness in g/cm<sup>2</sup> of the target, respectively.  $N_{\text{beam}}$  is the effective number of beam pions on the target including the DAQ efficiency.  $\Delta\Omega$  is the angular acceptance of the SKS spectrometer. An acceptance map of SKS in the 2-dimensional space of the momentum and the emission angle of  $K^+$  is estimated by a Monte Carlo simulation calculation based on GEANT4 package [28].  $\epsilon$  is the overall efficiency comes from detector and analysis efficiencies estimated from experimental data. The differential cross section is also derived as follows,

$$\frac{d\sigma}{d\Omega} = \frac{A}{N_A \rho x} \frac{N_K}{N_{\text{beam}} \Delta\Omega \epsilon}, \quad (2)$$

where  $N_K$  is the number of detected kaons, and  $N_K = \sum n_K$  where the summation runs over a spectral shape of signal events in the missing-mass spectrum.

To confirm the validity of the procedure of the cross section calculation, we estimated the cross section of the  $p(\pi^-, K^+)\Sigma^-$  reaction with the same method. Figure 4 shows the estimated differential cross section,  $d\sigma_{\text{cm}}/d\Omega$ , in the center of mass frame

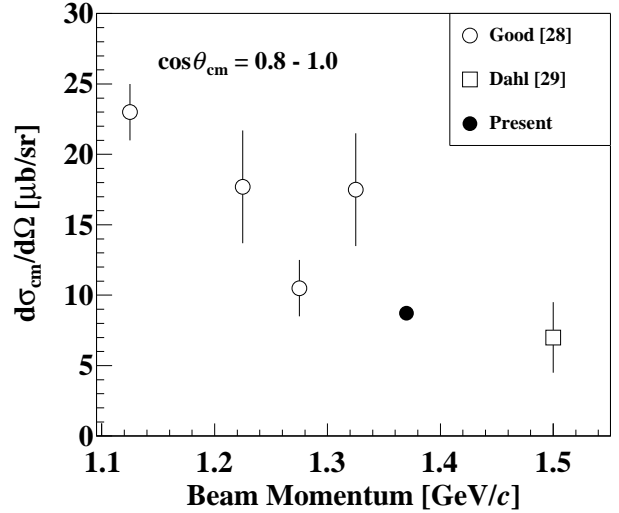


Figure 4: Differential cross section of the the  $p(\pi^-, K^+)\Sigma^-$  reaction in the center of mass frame as a function of the beam momentum. The open circles and the open box are the cross sections reported by Good et al. [29] and Dahl et al. [30], respectively. The full circle shows the present result.

(full circle) in the angular range of  $\cos\theta_{\text{cm}}=0.8-1.0$  together with the cross sections reported by Good et al. [29] (open circles) and Dahl et al. [30] (open box). The differential cross sections gradually decrease with the increase of the beam momentum, and the present result is consistent with the general trend.

Figure 5 shows the missing-mass spectrum of the <sup>6</sup>Li( $\pi^-$ ,  $K^+$ ) reaction. The vertical axis shows the double differential cross section in the laboratory frame averaged over the scattering angle from 2° to 14°,  $d^2\bar{\sigma}_{\text{lab}}/d\Omega/dM$  in a unit of nb/sr/(MeV/c<sup>2</sup>). The estimation of the spectrometer acceptance has small ambiguity in the selected angular range. The uncertainty of the missing-mass scale is  $\pm 1.26$  MeV/c<sup>2</sup> which is estimated from the beam momentum uncertainty  $\pm 1.34$  MeV/c. The continuum of the unbound  $\Lambda$  formation reaction and the component of the  $\Sigma^-$  quasi-free production reaction are observed in the missing-mass regions of 5810–5880 MeV/c<sup>2</sup> and above 5880 MeV/c<sup>2</sup>, respectively. A magnified view in the missing-mass range of 5795–5830 MeV/c<sup>2</sup> is shown in the inset. Around the  ${}^4_{\Lambda}\text{H}+2n$  particle decay threshold indicated by the arrow (5801.7 MeV/c<sup>2</sup>), no significant peak structure is observed.

As the first step of the calculation of an upper limit of the differential cross section,  $d\bar{\sigma}_{\text{lab}}/d\Omega$ , for a state of  ${}^6_{\Lambda}\text{H}$ , we estimated the number of observed events in the missing-mass re-

gion around the  ${}^4_{\Lambda}\text{H}+2n$  threshold. For the estimation of the number of events which associate to the production of a state, we set a missing-mass window of  $\pm 2\sigma$ , where  $\sigma$  is rms of the missing-mass resolution ( $\sigma = 1.36 \text{ MeV}/c^2$ ). There are 3 events in the threshold region within the missing-mass window. Therefore, we interpret the 3 events as observed events which include background and possible signal events.

Another necessary information for the upper limit estimation is the number of background events. Population of events are observed in the missing-mass region lower than  $5780 \text{ MeV}/c^2$  where we do not expect any physical backgrounds. The level of the event population averaged in the range from  $5700$  to  $5780 \text{ MeV}/c^2$  is  $(0.39 \pm 0.05)$  events per  $1 \text{ MeV}/c^2$ . These events are instrumental background due to particle miss-identifications, and a similar level of backgrounds are expected also at the  ${}^4_{\Lambda}\text{H}+2n$  threshold. The number of background events is estimated by multiplying the background level and the width of the missing-mass window.

If the Poisson statistics is used, the upper limit of the number of signal events is estimated to be 4.80 at 90% confidence level. Although we assume a flat distribution of the background events, the missing-mass dependence of the background level is not well known due to the low statistics. Therefore, we employ another upper limit of 6.68 events coming from the background free hypothesis as a conservative estimation.

As shown in Fig. 5, the differential cross sections are roughly  $0.1 \text{ nb}/\text{sr}$  per event for the observed 3 events. However, the differential cross sections largely depend on the observed scattering angles and may have a statistical bias. If an event happens to be observed at the forward angle, the cross section is underestimated, and vice versa, in our setup. To avoid the bias of the observation, we estimate the differential cross section averaged over the selected angular range, from  $2^\circ$  to  $14^\circ$ , and we obtain a value of  $0.18 \text{ nb}/\text{sr}$  for 1 event. By using the value, the upper limit of the differential cross section averaged in the scattering angle from  $2^\circ$  to  $14^\circ$  is estimated to be  $1.2 \text{ nb}/\text{sr}$  at 90% confidence level.

#### 4. Discussion

In our measurement, neither significant peak structure nor a large yield is observed around the  ${}^4_{\Lambda}\text{H}+2n$  particle decay threshold in the missing-mass spectrum of the  ${}^6\text{Li}(\pi^-, K^+)$  reaction. The  ${}^6_{\Lambda}\text{H}$  hypernucleus is believed to have the  ${}^4_{\Lambda}\text{H}+2n$  structure dominantly and to have the  $0^+$  ground and the  $1^+$  excited states which are analogous to the  $0^+$  and  $1^+$  spin-doublets in  ${}^4_{\Lambda}\text{H}$ . As far as the FINUDA result is concerned [21], the observed  ${}^6_{\Lambda}\text{H}$  candidate events were interpreted as the primary population of the excited  $1^+$  state by the  $(K^-_{\text{stopped}}, \pi^+)$  reaction followed by the  $\gamma$ -ray transition to the ground  $0^+$  state because the direct population of the  $0^+$  state should be suppressed due to the small spin-flip amplitude. The FINUDA results indicate that the excited  $1^+$  state, whose excitation energy is estimated to be  $1 \text{ MeV}$ , should be particle bound, otherwise the  $\gamma$ -ray transition to the  $0^+$  ground state should be impossible. If the  $1^+$  state is bound and the production cross section is comparable with that for  ${}^{10}\text{Li}$  of  $11.3 \text{ nb}/\text{sr}$ , more than 60 events should be observed

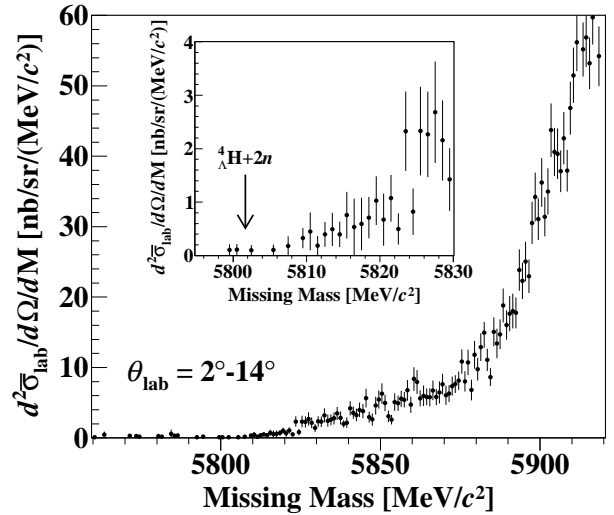


Figure 5: Missing-mass spectrum of the  ${}^6\text{Li}(\pi^-, K^+)$  reaction at  $1.2 \text{ GeV}/c$ . The ordinate shows the double differential cross section averaged over the angular range from  $2$  to  $14$  degrees. A magnified view around the  $\Lambda$  bound region is shown in the inset. The arrow labeled as  ${}^4_{\Lambda}\text{H}+2n$  shows the particle decay threshold ( $5801.7 \text{ MeV}/c^2$ ).

as a peak in the  $\Lambda$  bound region in the missing-mass spectrum of the  ${}^6\text{Li}(\pi^-, K^+)$  reaction. Therefore, our observation is in conflict with the simple interpretation of the FINUDA observation.

Hiyama et al. [15] suggested that the both  $0^+$  and  $1^+$  states are unbound. If it is the case, production cross sections may be smaller than the sensitivity of our measurement due to the broad wave-functions of the unbound states which have small overlaps with the wave-function in the initial  ${}^6\text{Li}$  nucleus. Gal and Millener [14] discussed another possible interpretation of the FINUDA observation. They suggested a possibility of an unbound  $1^+$  state, whose particle decay width is extremely small and comparable with that of the  $M1 \gamma$  decay to the ground  $0^+$  state due to kinematical and dynamical suppression of the emission of two neutrons from the  $1^+$  excited state. The FINUDA collaboration also discussed another scenario for the spectrum of  ${}^6_{\Lambda}\text{H}$  in which two out of the three candidate events came from the population of the spin-triplet states,  $1^+$ ,  $2^+$  and  $3^+$ , at around  $3 \text{ MeV}$  excitation [31]. Therefore, it is interesting to compare our upper limit,  $1.2 \text{ nb}/\text{sr}$ , with quantitative theoretical estimations of the production cross sections because the cross sections are sensitive to the binding energies and the wave-functions of the low-lying states.

#### 5. Summary

We performed the measurement of the  ${}^6\text{Li}(\pi^-, K^+)$  reaction at the beam momentum of  $1.2 \text{ GeV}/c$ . No significant peak structure is observed around the  ${}^4_{\Lambda}\text{H}+2n$  threshold. The upper limit of the differential cross section in the scattering angle from  $2^\circ$  to  $14^\circ$  is estimated to be  $1.2 \text{ nb}/\text{sr}$  at the 90% confidence level. The result does not favor the simple interpretation of the FINUDA observation and it suggests reconsideration of the structure of

the  ${}^6_{\Lambda}\text{H}$  hypernucleus. More clear insight of the  ${}^6_{\Lambda}\text{H}$  structure may be obtained by comparing our cross section upper limit with quantitative theoretical calculations.

## Acknowledgements

We would like to acknowledge the staff of the Hadron beam line and J-PARC accelerator groups for their efforts of improving the beam quality and keeping the stable operation during the beam time. We also thank Professors Y. Akaishi, T. Harada, A. Gal and E. Hiyama, for the fruitful discussions. The experiment was supported by the Grant-in-Aid for Scientific Research (KAKENHI), for Scientific Research on Innovative Areas No. 24105003, for Young Scientist (A) No. 23684011, for Basic Research (Young Researcher) No. 2010-0004752 from National Research Foundation in Korea and for Scientific Research (C) No. 24540305 from the Ministry of Education, Culture, Sports, Science and Technology in Japan. We acknowledge support from WCU program, National Research Foundation, Center for Korean J-PARC Users, and the Ministry of Education, Science, and Technology (Korea).

## References

- [1] M. Danysz and J. Pniewski, *Philos. Mag.* **44** (1953) 348.
- [2] W. Brückner, et al., *Phys. Lett. B* **55** (1975) 107.
- [3] M. May et al., *Phys. Rev. Lett.* **47** (1981) 1106.
- [4] P.H. Pile et al., *Phys. Rev. Lett.* **66** (1991) 2585.
- [5] H. Hotchi et al. (KEK E369 Collaboration), *Phys. Rev. C* **64** (2001) 044302.
- [6] H. Tamura et al. (KEK E419 Collaboration), *Phys. Rev. Lett.* **84** (2000) 5963.
- [7] S. Ajimura et al. (BNL E929 Collaboration), *Phys. Rev. Lett.* **86** (2001) 4255.
- [8] M. Ukai et al. (BNL E930 Collaboration), *Phys. Rev. C* **77** (2008) 054315.
- [9] B.F. Gibson, A. Goldberg and M.S. Weiss, *Phys. Rev. C* **6** (1972) 741.
- [10] Y. Akaishi, T. Harada, S. Shinmura, Khin Swe Myint, *Phys. Rev. Lett.* **84** (2000) 3539.
- [11] R.H. Dalitz and R. Levi Setti, *Nuovo Cimento* **30** (1963) 489.
- [12] A.A. Korshennikov et al., *Phys. Rev. Lett.* **87** (2001) 092501.
- [13] Y. Akaishi and T. Yamazaki, *Frascati Physics Series XVI* (1999) 59.
- [14] A. Gal and D.J. Millener, *Phys. Lett. B* **725** (2013) 445.
- [15] E. Hiyama et al., *Nucl. Phys. A* **908** (2013) 29.
- [16] L. Majling, *Nucl. Phys. A* **585** (1995) 211c.
- [17] K. Kubota et al., *Nucl. Phys. A* **602** (1996) 327.
- [18] P.K. Saha et al. (KEK E521 Collaboration), *Phys. Rev. Lett.* **94** (2005) 052502.
- [19] T. Harada, A. Umeya and Y. Hirabayashi, *Phys. Rev. C* **79** (2009) 014603.
- [20] M. Agnello et al. (FINUDA Collaboration), *Phys. Lett. B* **640** (2006) 145.
- [21] M. Agnello et al. (FINUDA Collaboration), *Phys. Rev. Lett.* **108** (2012) 042501.
- [22] T. Takahashi et al., *Prog. Theor. Exp. Phys.* **2012** (2012) 02B010.
- [23] T. Fukuda et al., *Nucl. Instrum. Methods A* **361** (1995) 485.
- [24] R. Honda and K. Miwa, *Proceedings of 3rd International Workshop on New Photon-Detectors*, PoS Press, Orsay, 2012, p.031.
- [25] Y. Igarashi et al., *IEEE Trans. Nucl. Sci.* **57** (2010) 618.
- [26] Y. Ma et al. (KEK E566 Collaboration), *Nucl. Phys. A* **835** (2010) 422.
- [27] K. Hosomi et al. (KEK E566 Collaboration), *Nucl. Phys. A* **914** (2013) 184.
- [28] CERN Program Library Entry W5013, GEANT.
- [29] M.L. Good and R.R. Kofler, *Phys. Rev.* **183** (1969) 1142.
- [30] O.I. Dahl et al., *Phys. Rev.* **163** (1967) 1430.
- [31] M. Agnello et al. (FINUDA Collaboration), *Nucl. Phys. A* **881** (2012) 269.